Check for updates

Novel skin defense peptides and microbiota contribute to disease resilience of the Ngäbe-Buglé leopard frog

Douglas C. Woodhams[1,2]*, Aura Muñiz-Torres[1†], Andreas Hertz[1],
Patrick Kearns[1], Nina McDonnell[1], Laura Reinert[3],
Louise A. Rollins-Smith[3,4], Brandon LaBumbard[1], Jamie Voyles[5],
Corinne L. Richards-Zawacki[6], Daniel Callahan[1]
and J. Michael Conlon[7]

[1]Biology Department, University of Massachusetts Boston, Boston, MA, United States, [2]Smithsonian Tropical Research Institute, Panama City, Panama, [3]Department of Pathology, Microbiology and Immunology, Vanderbilt University School of Medicine, Nashville, TN, United States, [4]Department of Biological Sciences, Vanderbilt University, Nashville, TN, United States, [5]Department of Biology, University of Nevada Reno, Reno, NV, United States, [6]Department of Biological Sciences, University of Pittsburgh, Pittsburgh, PA, United States, [7]Diabetes Research Centre, School of Biomedical Sciences, Ulster University, Coleraine, United Kingdom

Some of the amphibian populations in Panama are demonstrating slow recovery decades after severe declines caused by the invasion of the fungal pathogen *Batrachochytrium dendrobatidis* (*Bd*). However, new species remain to be described and assessed for the mechanisms of disease resilience. We identified seven skin defense peptides from a presumably novel leopard frog species in the Tabasará range, at Buäbti (Llano Tugrí), Ngäbe-Buglé Comarca, and Santa Fe, Veraguas, Panama, herein called the Ngäbe-Buglé leopard frog. Two of the peptides were previously known: brevinin-1BLb from *Rana (Lithobates) blairi* and a previously hypothesized "ancestral" peptide, ranatuerin-2BPa. We hypothesized that the peptides are active against *Bd* and shape the microbiome such that the skin bacterial communities are more similar to those of other leopard frogs than of co-occurring host species. Natural mixtures of the collected skin peptides showed a minimum inhibitory concentration against *Bd* of 100 µg/ml, which was similar to that of other leopard frogs that have been tested. All sampled individuals hosted high intensity of infection with *Bd*. We sampled nine other amphibian species in nearby habitats and found lower prevalence and intensities of *Bd* infection. In addition to the pathogen load, the skin microbiomes were examined using 16S rRNA gene targeted amplicon sequencing. When compared to nine co-occurring amphibians, the Ngäbe-Buglé leopard frog had similar skin bacterial richness and anti-*Bd* function, but the skin microbiome structure differed significantly among species. The community composition of the bacterial skin communities was strongly associated with the *Bd* infection load. In contrast, the skin microbiome composition of the Ngäbe-Buglé leopard frog was similar to that of five North American leopard frog populations and the sympatric and congeneric *Rana (Lithobates) warszewitschii*, with 29 of the 46 core bacteria all demonstrating anti-*Bd* activity in culture. Because of the high *Bd* infection load and prevalence

in the Ngäbe-Buglé leopard frog, we suggest that treatment to reduce the *Bd* load in this species might reduce the chytridiomycosis risk in the co-occurring amphibian community, but could potentially disrupt the evolution of skin defenses that provide a mechanism for disease resilience in this species.

Introduction

Understanding the host immune function is increasingly important at a time when emerging infectious diseases rise to the forefront of global concerns (Rohr et al., 2023; Pfenning-Butterworth et al., 2024). Amphibians have gained prominence as valuable model species in immunology for multiple reasons. Although many components of the amphibian immune system are highly conserved among vertebrates, the diversity of immunological responses among amphibian host species provides insights into susceptibility to disease and the generation of infection resistance or tolerance mechanisms (Assis et al., 2023; Ruiz and Robert, 2023). In addition, infectious diseases—specifically the disease chytridiomycosis—have been implicated in severe declines in amphibian populations and species around the world (Wake and Vredenburg, 2008; Scheele et al., 2019). As such, a better understanding of the immune defenses of amphibians can make meaningful contributions to the fields of immunology and microbial and disease ecology and to the study of infectious disease in general (Assis et al., 2023; Ruiz and Robert, 2023).

The fungal pathogens that cause chytridiomycosis, *Batrachochytrium dendrobatidis* (*Bd*) and *Batrachochytrium salamandrivorans* (*Bsal*), were first described in 1998 and 2014, respectively (reviewed in Woodhams et al., 2018). Renowned for its ability to spread rapidly through naive amphibian communities around the world, *Bd* causes mass mortality events and even the complete extinction of host species (Valenzuela-Sánchez et al., 2017). No other pathogen is known to have had such a ubiquitous effect on such a broad range of host species and in so many different environments (Lips, 2016). Similarly, *Bsal* is poised to greatly impact naive populations of amphibians (Castro Monzon et al., 2022), particularly in the Americas (Gray et al., 2023).

The amphibian declines that occurred in the tropical mountains of Central America provide an excellent system for investigating the links between species loss and ecosystem function. In this region, a west-to-east spread of *Bd* was incontrovertibly linked to population declines and die-offs and resulted in dramatic losses of amphibian biodiversity (Lips et al., 2006; Crawford et al., 2010). Since the initial epizootic events, some species have shown evidence of recovery, even though *Bd* is now pervasive (i.e., enzootic) (Voyles et al., 2018;

Hollanders et al., 2023). The epizootic–enzootic transition represents a significant change in the disease dynamics, but does not mean the threat has abated (Catenazzi et al., 2017). Our research in this area has revealed that the epizootic–enzootic transition is not due to pathogen attenuation as *Bd* is still highly lethal in these host assemblages. Rather, recent results have suggested that changes in the host defenses, not the pathogen, could be driving the epizootic–enzootic shift in the chytridiomycosis system in this region (Voyles et al., 2018).

Both skin defense peptides and the skin microbiome, among other defenses, could act to inhibit the pathogen *Bd* (Woodhams et al., 2018). In the leopard frogs *Rana pipiens* and *Rana sphenocephala*, skin peptides are an effective immune defense against *Bd* and perhaps other pathogens (Le Sage et al., 2021). Both the skin defense peptides and skin microbiomes shift seasonally in these species, cycling consistent with the dynamics of infection risk.

The northern leopard frog, *R. pipiens*, has been a focal system for the study of skin defense peptides because it is a wide-ranging and historically abundant species (Woodhams et al., 2008; Tennessen et al., 2009; Tennessen and Blouin, 2010; Pask et al., 2012). As a species complex (*Rana* subgroup clade 9 *Panthera*) (Yuan et al., 2016), the leopard frogs range from Northern Canada to Panama, and new, sometimes cryptic, species have been described in recent years (Pfeiler and Markow, 2008; Newman et al., 2012; Luque-Montes et al., 2018). While the Ngäbe-Buglé leopard frogs studied here have been previously studied (e.g., perhaps *Rana* species 4 in Hillis and Wilcox, 2005; or *Lithobates pipiens* sp. 'E' in Brem and Lips, 2008), they have not been formally described. However, specimens are archived in the American Museum of Natural History A-124167: Panama: Chiriquí: 9 km SSE El Volcán (GenBank AY779245) and by AH at the Senckenberg Natural History Museum (Frankfurt, Germany). Morphological and genetic assessments placed the specimens in a novel species (DCW, AH, Dudek, and Townsend, unpublished data), distinct from any other Ranidae that occur in Panama or Costa Rica and currently under evaluation.

In this study, we characterized an understudied species, the Ngäbe-Buglé leopard frog. We used peptidomics and described the peptide defenses against *Bd* and *Bsal*. Because peptides from other

well-studied leopard frogs produce strong antifungal skin peptide defenses, we hypothesized that the Ngäbe-Buglé leopard frog would produce similar bioactive skin peptides that also shape the microbiome. We hypothesized that the skin microbiome of this species would be more similar to those of other leopard frogs compared with the more distantly related amphibian species sampled from the same locality.

A previously hypothesized ancestral Ranatuerin-2 peptide of *R. pipiens* and *R. blairi* was suspected to have undergone a selective sweep. While previously hypothetical, we found this peptide in the Ngäbe-Buglé leopard frogs. We investigated the possible involvement of chytridiomycosis in the selective sweep described by Tennessen and Blouin (2010) by synthesizing peptides and testing their activity against *Bd* and Bsal, comparing the anti-*Bd* activity of the ancestral and extant peptides. We quantified the *Bd* infection loads and prevalence in the Ngäbe-Buglé leopard frogs compared with sympatric species in Panama and compared this with the skin microbiomes. Disease mitigation recommendations are provided based on these results.

Materials and methods

Field sampling

In January of 2016 and 2018, amphibians were sampled at Alto de Piedra, which is located at the border of Santa Fe National Park, along rainforest trails and in ponds (Brem and Lips, 2008; Figure 1). The sample types for each species are indicated in Table 1, in addition to the mean body size, *Bd* and *Bsal* infection diagnostics, and activity against *Bd* (JLV Campana isolate).

Collection and purification of skin peptides and structural characterization

Skin defense peptides were collected from the focal species, the Ngäbe-Buglé leopard frog, and comparative skin peptide profiles (MALDI mass spectra) were produced from *Espadarana prosoblepon*, *Hyloscirtus colymba*, and *R. warszewitschii*, as indicated in the Supplementary Material (Supplementary Figure S1) alongside images of the species sampled. The skin peptides were released by a subcutaneous injection of 40 nmol/g body mass of norepinephrine (bitartrate salt; Sigma, St. Louis, MO, USA) in amphibian phosphate-buffered saline and the secretions collected in 23 ml sterile Millipore Milli-Q water for 15 min as previously described (Woodhams et al., 2006). The peptide secretions were acidified in the field to 1% volume in hydrochloric acid and were collected on methanol-activated Sep-Pak C-18 cartridges. After partial purification and elution from the Sep-Pak C-18 cartridges in 70% acetonitrile, the freeze-dried skin secretion (approximately 4 mg) was redissolved in 0.1% (v/v) trifluoroacetic acid (TFA)/water (1 ml) and the combined sample injected onto a semi-preparative (1.0 cm × 25 cm) Vydac 218TP510 (C-18) reversed-phase high-performance liquid chromatography
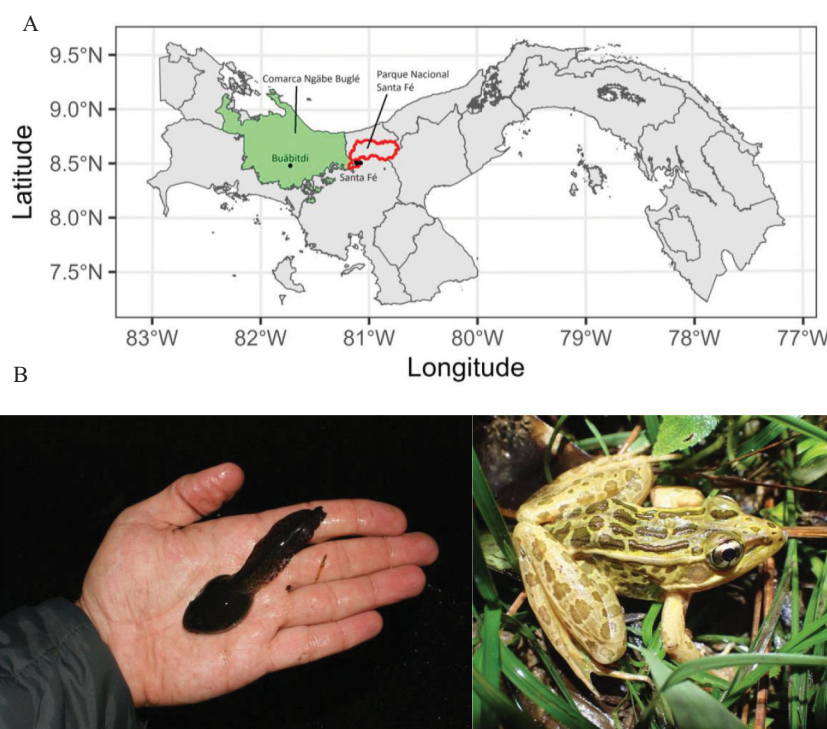
FIGURE 1
Ngäbe-Buglé leopard frogs in Panama. **(A)** Range likely includes the Tabasará Mountains (three known sites indicated by *black dots* at elevation of 1,300−860 m asl; Comarca Ngäbe-Buglé in *green* and Parque National Santa Fe in *red*). **(B)** Photo of a tadpole from Buäbitdi, the capital of Comarca Ngäbe-Buglé, on March 23, 2009, taken by AH and of an adult frog from near Alto de Piedra, Santa Fe, taken in January 2018 by DCW. In 2009, field notes indicated that there where many dead recently metamorphosed juveniles at the site. Most living juveniles had difficulty moving and showed very swollen reddish hind limbs. Monitoring of this range-restricted species is needed to better determine the population trends, disease threats, and life history.

TABLE 1   Samples from frogs at Alto de Piedra near Santa Fe, Panama.

Species	n (microbiome analysis)	n (pathogen diagnostics)	n (mucosome function against Bd)	Mean mass g (SD)	mean Log (Bd load)	Max Log (Bd)	Proportion Bsal infected	Proportion Bd infected	mean mucosome Bd inhibition *	SE (mucosome)	mean mucosome Bd inhibition per cm2 surface area*	SE (mucosome/ SA)
Craugastor crassidigitus	10	10	6	5.9 (3.4)	0.89	3.37	0	0.40	10.98	4.17	0.57	0.22
Espadarana prosoblepon	16	16	16	1.0 (0.1)	0.23	1.94	0	0.19	-1.44	3.00	-0.16	0.31
Hyloscirtus colymba (adults)	21	20	20	2.2 (0.4)	0.52	3.05	0	0.15	12.64	3.12	0.83	0.20
Hyloscirtus colymba (tadpoles)	3	11	0	nd	1.39	4.65	0	0.36	nd	nd	nd	nd
Rana (Lithobates) warszewitschii	9	9	10	4.1 (0.9)	0.73	5.90	0	0.17	11.77	4.08	0.60	0.18
Ngäbe-Buglé leopard frog	13	13	13	22.3 (11.1)	3.75	7.57	0	1.00	11.43	3.78	0.21	0.07
Pristimantis cerasinus	4	4	1	0.8 (1.0)	0.73	1.51	0	0.75	29.68		1.93	
Pristimantis museosus	3	2	0	nd	0.00	0.00	0	0.00	nd	nd	nd	nd
Pristimantis pardalis	3	3	3	1.5 (0.9)	2.04	5.30	0	0.67	11.84	3.48	0.99	0.22
Sachatamia albomaculata	3	3	1	1	0.19	0.56	0	0.33	44.48		4.62	
Smilisca sila	4	3	0	nd	0.00	0.00	0	0.00	nd	nd	nd	nd
Sum	89	94	70					0.362				

Individual data available in github repository at: https://github.com/pattyjk/Woodhams_et_al_Front_AmphRep.

Nd, not determined

*Negative value indicates that *Batrachochytrium dendrobatidis* (*Bd*) growth was facilitated by the addition of mucosome.
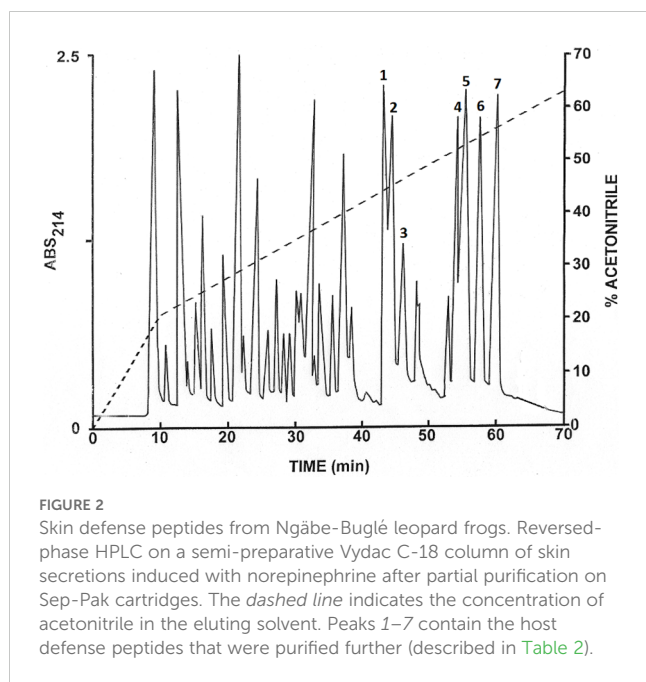
FIGURE 2
Skin defense peptides from Ngäbe-Buglé leopard frogs. Reversed-phase HPLC on a semi-preparative Vydac C-18 column of skin secretions induced with norepinephrine after partial purification on Sep-Pak cartridges. The *dashed line* indicates the concentration of acetonitrile in the eluting solvent. Peaks *1–7* contain the host defense peptides that were purified further (described in Table 2).

(HPLC) column (Grace, Deerfield, IL, USA) equilibrated with 0.1% (*v/v*) TFA/water at a flow rate of 2.0 ml/min. The concentration of acetonitrile in the eluting solvent was raised to 21% (*v/v*) over 10 min and to 63% (*v/v*) over 60 min using linear gradients. Absorbance was monitored at 214 nm and the fractions (1 min) collected using a BioRad 2110 fraction collector.

Aliquots (20 µl) of the peaks that were present in major abundance with retention times >40 min were analyzed using electrospray ionization (ESI) mass spectrometry (MS). The peaks designated 1–7 in Figure 2 contained components with molecular masses in the range 2–3 kDa. These peptides were subjected to further purification by successive chromatographies on (1.0 cm × 25 cm) Vydac 214TP510 (C-4) and (1.0 cm × 25 cm) Vydac 208TP510 (C-8) columns. The concentration of acetonitrile in the eluting solvent was raised from 21% to 56% (*v/v*) over 50 min at a flow rate of 2.0 ml/min.

ESI-MS was carried out at Vanderbilt University Medical Center using a Thermo Orbitrap XL mass spectrometer equipped with an *Ion Max* standard electrospray ion source (see Supplementary Material for additional methodological details). The primary structures of the purified peptides were determined by automated Edman degradation using a model 494 Procise sequenator (Applied Biosystems, Foster City, CA, USA) following the manufacturer's recommended protocol.

Testing natural peptide mixtures and synthetic peptides against pathogens

Growth inhibition assays were used to determine the minimum inhibitory concentration (MIC), or the lowest concentration at which microbial growth was completely inhibited, of natural peptide mixtures from the Ngäbe-Buglé leopard frogs against *Bd* (JEL197 isolate) following the methods of Rollins-Smith et al. (2002). Briefly, the purified natural mixture was prepared in an eight-part 50% serial dilution series ranging from 500 to 3.13 µg/ml. The *Bd* isolate JEL-197 zoospores were plated in 1% tryptone broth (5×10^6/well in 50 µl) in 96-well flat-bottomed microtiter plates (Costar 3596, Corning, Corning, NY, USA), with or without serial dilutions of peptides in sterile HPLC-grade water in a volume of 50 µl (final volume, 100 µl/well). Cultures were grown for 7 days at 22°C. The peptides were filter-sterilized and were each plated in five replicates along with heat-killed zoospores in negative control wells, with no peptide in positive control wells. Growth was measured as an increase in optical density at 490 nm using a microtiter plate reader (BioTek ELx808 machine, Agilent Technologies, Santa Clara, CA, USA). The MIC was calculated as the lowest concentration at which growth was not detectable (not significantly greater than the negative control).

Subsequently, the individually synthesized peptides were tested against *Bd* (strain from Campana, Panamá) and *Bsal* (*Bsal* 2.0 strain provided by Frank Pasmans). The *Bd* strain from Campana was selected as it originates from the same region where the Ngäbe-Buglé leopard frogs were found. The newly described peptides (Table 2), along with the previously studied ranatuerin-2P for

TABLE 2 Primary structures and molecular masses of the peptides isolated from norepinephrine-stimulated skin secretions and the closest related amphibian antimicrobial peptides (AMPs).

Peptide (min)	Primary Structure	Proposed Name (NB: Ngäbe- Buglé)	$[M^+]$ obs	$[M^+]$ calc	Similarity (%, described peptide, species)
1 (45.1)	GLMDTVKNAAKNLAGQMLDKLKCKITGC	Ranatuerin-2BPa Ancestral peptide from Tennessen & Blouin (2010)	2961.5	2961.5	96.55 (Ranatuerin-2Ona, *Rana onca*)
2 (45.2)	GLMDTVKGVAKTVAASMLDKLKCKITGC	Ranatuerin-2NB	2878.5	2878.5	92.86 (Ranatuerin-2VEb, *Odorrana versabilis*; Ranatuerin-2Ya, *Lithobates yavapaiensis*)
3 (45.3)	FLPIIAGM(O)AAKVLPKIFCAISKKC	[Met(0)^8]brevinin-1NBb	2575.4	2575.5	
4 (54.1)	FLPVIAGMAAKFLPKIFCAISKKC	Brevinin-1NBa	2593.4	2593.5	95.65 (B1CTcu4, *Clinotarsus curtipes*)
5 (54.2)	FLPIIAGMAAKVLPKIFCAISKKC	Brevinin-1NBb	2559.4	2559.5	95.83 (Brevinin-1BLb, *Lithobates blairi*)
6 (57.1)	FLPIIAGVAAKVLPKIFCAISKKC	Brevinin-1BLb	2527.5	2527.5	100 (Brevinin-1BLb, *Lithobates blairi*)
7 (57.2)	FLPIIAGMAANVLPKIFCAISKKC	Brevinin-1NBc	2545.4	2545.5	91.67 (Brevinin-1BLb, *Lithobates blairi*)

$[M^+]_{obs}$ denotes the observed molecular mass, while $[M+]_{calc}$ represents the molecular mass calculated from the proposed structures.

comparison, were synthesized by PeptideSyn (LifeTein, Somerset, NJ, USA) with C-terminal cystine disulfide bridges. The synthetic products were first hydrated in 4% sterile TFA to maximize the compound solubility, then ultrapure water was gradually added over several minutes to achieve final stock concentrations of 1 mM peptide and 0.1% TFA. To prepare the highest peptide concentration used in assays, peptide stocks were diluted 2:8 in ultrapure water (Milli-Q), yielding concentrations of 200 µM peptide and 0.02% TFA. Thus, a six-part 50% serial dilution series of each synthetic peptide was prepared in 0.02% sterile TFA to standardize the acid concentration across the series. MIC assays were prepared in an optically clear flat-bottomed 96-well plate: each well was prepared with 100 µl diluted peptide or sterile 0.02% TFA as a control, in triplicate. Subsequently, each well was inoculated with 100 µl 1×10^6 Bd or Bsal zoospores in 1% tryptone broth using heat-killed zoospores to control for background absorbance. The resulting peptide concentrations that were used to determine the MICs for Bd and Bsal were 100, 50, 25, 12.5, 6.25, and 3.13 µM, all with a final well concentration of 0.01% TFA. Plates were wrapped in parafilm to prevent evaporation and were incubated at constant temperatures (23°C for Bd and 15°C for Bsal). The optical density at 490 nm was measured immediately after plate setup on day 0, then on days 4, 6, and 7. Independent t-tests were conducted to assess the effectiveness of the peptide concentrations in inhibiting the growth of Bd and Bsal compared with their respective heat-killed controls. Subsequently, effect sizes were calculated using Cohen's d to quantify the magnitude of the differences observed in the t-tests and to determine the MIC that was not different from the heat-killed control.

Mucosome activity against Bd

The mucosome ("mucos-ome," a similar concept to other omics) is the bioactive skin surface of amphibians consisting of mucin proteins and other secreted host products and the microbiome (microbial community and metabolites) (Woodhams et al., 2014). It is sometimes referred to as the dermosphere (Assis et al., 2017; Brunetti et al., 2023). The mucosome may also contain constitutively expressed peptides, on amphibians that produce them (Pask et al., 2012; Woodhams et al., 2016). Skin mucosome samples were collected from the amphibians listed in Table 1 by rinsing them for 60 min in 15 ml water and then freezing the sample directly. Samples were frozen and transported to the lab, then aliquots were used to evaluate their capacity to inhibit Bd growth (Campana isolate) according to previously published methods (Woodhams et al., 2014). We report activity per square centimeter surface area in comparison to negative and positive controls. Negative controls were heat-killed zoospores, while positive controls were zoospores exposed to vehicle only, absent mucosome samples. Mucosome activity was tested for correlation with the proportion of the microbiome reads matching anti-Bd bacteria, for correlation with the anti-Bd bacterial richness, and for correlation with the Bd infection loads (individuals) and prevalence of infection (species).

Quantification of Batrachochytrium dendrobatidis infection

DNA was extracted from swabs using 40 µl of PrepMan and the abundance of Bd and Bsal was measured using quantitative polymerase chain reaction (qPCR) according to the methods in Blooi et al. (2013). Briefly, the samples were amplified in duplicate 20 µl reactions with the following chemistry: 3.42 µl PCR grade water, 0.46 µl ITS1-3 Chytr (5′-CCTTGATATAATACAGTGTGCCATATGTC-3′), 0.46 µl 5.8S Chytr (5′-TCGGTTCTCTAGGCAACAGTTT-3′), 0.645 µl Bd probe (MGB2 5′-CGAGTCGAAC-3′), and 5 µl DNA template. The reactions were performed with the following cycling conditions for 50 cycles: denaturation at 95°C for 15 s, followed by 20 s at 60°C, and 72°C for 30 s. The copy number of Bd ITS was calculated using either a plasmid (USA species) or a gBlock (Panama species) standard curve.

Metagenomic DNA extraction and sequencing library preparation

DNA for metagenomics was extracted from skin swabs preserved in 50 µl DNA/RNA Shield using the Qiagen Blood and Tissue DNA Isolation Kit (Qiagen, Hilden, Germany), with the addition of a 1-h lysozyme incubation at 37°C at the start of the protocol. The bacterial portion of the microbiome was characterized using the primer pair 515F/806R following protocols of the Earth Microbiome Project (Caporaso et al., 2012; Thompson et al., 2017; Parada et al., 2016). Each sample was amplified in 25 µl duplicate reactions with the following chemistry: 11 µl of PCR-grade water, 10 µl of PCR master mix (Axura Red mix, Azura Genomics, Raynham, MA, USA), 1 µl of 10 µM forward and reverse primers, and 2 µl of undiluted DNA template. DNA was amplified using the following conditions: 94°C for 3 min, followed by 29 cycles of 94°C for 45 s, 50°C for 60 s, and 72°C for 90 s, with a final extension at 72°C for 10 min. In addition to amplifying the DNA from the microbiome swabs, we included a PCR-negative extraction control and a swab-negative control to remove potential contaminants following sequencing. The PCR products were verified via electrophoresis and each sample was pooled prior to purification using the ThermoFisher Scientific GeneJET PCR Purification Kit (ThermoFisher Scientific, Waltham, MA, USA). The DNA concentration was quantified using a NanoDrop spectrophotometer (Thermo Scientific NanoDrop 2000 Spectrophotometer) and pooled in equimolar amounts for paired-end sequencing on an Illumina MiSeq using a v2 300 cycle kit at the University of Massachusetts Boston.

Microbiome analyses

In addition to comparing the microbiome and Bd loads among the amphibian community at Alto de Piedra (Table 1), we compared the Ngäbe-Buglé leopard frog microbiomes with those from five populations of North American leopard frogs: R. blairi (n = 41 from New Mexico), R. sphenocephala (n = 94 from

Louisiana and $n = 80$ from Tennessee), and *R. pipiens* ($n = 49$ from Vermont and $n = 95$ from Pennsylvania). This leopard frog dataset (SERDP dataset) will be analyzed in greater detail elsewhere; here, we examined whether the core microbiome of the focal species is more similar to that of the North American or sympatric congeners, in particular the co-occurring *R. warszewitschii*, the closest co-occurring relative to the leopard frog (*Pantherana*) species group (Yuan et al., 2016).

Raw sequencing data were quality filtered and demultiplexed using QIIME2 (Bolyen et al., 2019). The sequences were clustered into sub-operational taxonomic units (sOTUs) using deblur (Amir et al., 2017). The sOTU contaminants detected in the PCR, swab, and extraction controls were also filtered prior to subsequent analysis. The samples were rarified to the lowest sampling depth (2,900 sequences per sample), and QIIME2 was used to calculate the alpha diversity (richness) and beta diversity with unweighted UniFrac (Lozupone and Knight, 2005). Other metrics showed similar results, but unweighted UniFrac tends to best differentiate the amphibian skin microbiomes. Taxonomy was assigned using Greengenes (v. 13.8) (McDonald et al., 2012). A non-parametric permutational multivariate analysis of variance (PERMANOVA) (Dixon, 2003) was used with 10,000 permutations to compare the community composition among species, locations sampled, and seasons for all leopard frogs, as well as for comparison among species for Panamanian amphibians. Spearman's correlation was used to delineate the impacts of *Bd* abundance by qPCR (see below for methods) and community composition [axis 1 values from the principal coordinates analysis (PCoA)].

The bacterial richness and the proportion of predicted anti-*Batrachochytrium* sOTUs were calculated. The latter was determined by matching the sOTUs to the 2023 version of the Antifungal Isolates Database (https://github.com/AmphiBac/AmphiBac-Database) (Woodhams et al., 2015) with vsearch (Rognes et al., 2016). Welch's *t*-test with a Benjamini–Hochberg corrected *p*-value was used for multiple comparisons to test for significant differences in the anti-*Batrachochytrium* abundance and sOTU richness. Finally, taxa that were important members of the microbiome across North American leopard frog populations and the Panamanian *R. warszewitschii* and Ngäbe-Buglé leopard frogs were examined by determining an occupancy/abundance relationship. We defined the important sOTUs by those that were either very abundant (>15% of the community) or had high occupancy (found in >50% of the samples).

The sequencing data were deposited in the NCBI Sequence Read Archive under accession numbers SRA PRJNA1175825 (Panama samples) and SRA PRJNA1177182. These are also available at https://github.com/pattyjk/Woodhams_et_al_Front_AmphRep.

Results

Field sampling

We sampled frogs comprising adults and subadults of ten species (Table 1 and Supplementary Figure S1), and tadpoles of *H. colymba*. In 2018, we sampled 13 adults of the focal species, here

called the Ngäbe-Buglé leopard frog. In 2009, AH previously sampled adults and juveniles at Buäbitdi in the Comarca Ngäbe-Buglé (Figure 1). Samples from both locations were genetically different from other Central American *Rana* based on the amphibian 16S sequences indicating an undescribed species (DCW, AH; Dudek and Townsend, unpublished data). We are not aware of how far this species ranges outside of the sampled sites, and the lack of a formal species description makes identifications (i.e., *Rana taylori* in iNaturalist) problematic. Myers and Duellman (1982) noticed that different species in the Serranía de Tabasará mountain range east of Fortuna and suggested that the low Fortuna depression acted as a barrier for highland species.

Purification of skin peptides and structural characterization

We chromatographed the skin secretions of the Ngäbe-Buglé leopard frog, after partial purification on methanol-activated Sep-Pak C-18 cartridges, on a Vydac C-18 semipreparative reversed-phase HPLC column (Figure 2). Peptides in the prominent peaks in the chromatogram with retention times > 40 min were purified to near homogeneity (purity > 98%), as assessed by a symmetrical peak shape and mass spectrometry, by further chromatography on semipreparative Vydac C-4 and Vydac C-8 columns (chromatograms not shown). Using ESI mass spectrometry, we established that the molecular masses in the peaks designated 1-7 were in the range 2-3 kDa. In subsequent structural analysis, we demonstrated that Peak 1 contained ranatuerin-2BPa, peak 2 ranatuerin-2NB, peak 3 [Met(0)^8]brevinin-1NBb, peak 4 brevinin-327 1NBa, peak 5 brevinin-1NBb, peak 6 brevinin-1BLc (previously described from *R. blairi*), and peak 7 brevinin-1NBc. The nomenclature follows generally accepted guidelines adopted for the host-defense peptides from frogs from the family Ranidae (Conlon, 2008). We give the suffix NB (for Ngäbe-Buglé leopard frog) to peptides identified as belonging to previously described families, and denote isoforms by lower case letters.

We established the primary structures of the peptides isolated from the skin secretions by automated Edman degradation and show their complete primary structures in Table 2. The monoisotopic molecular masses of the purified peptides determined by ESI mass spectrometry were consistent with the proposed structures and demonstrate that all peptides contained a disulphide-bridged cyclic domain in their C-terminal regions. The peptide present in peak 3 (Figure 2) represents the methionine-sulfoxide form of brevinin-1NBb.

Mucosome activity against *Bd*

Mucosome activity is summarized in Table 1 for all Panama amphibian species tested. No significant correlation was detected between the mucosome activity against *Bd* and the proportion of bacterial reads with anti-*Bd* function. Mucosome activity (without and with surface area correction) was not correlated with the *Bd* infection load across the individuals sampled, nor with the percent anti-*Bd* bacterial richness of the anti-*Bd* bacteria (Spearman's ρ =

−0.05 for percent inhibition and −0.15 for richness), and the mean mucosome activity per species was not correlated with *Bd* infection prevalence ($r = −0.22$, $p = 0.43$).

Testing natural peptide mixtures and synthetic peptides against pathogens

The natural mixture of skin defense peptides (Figure 3A) was active against *Bd* (type isolate JEL 197 with a MIC of 100 μg/ml) (Figure 3B). A summary of the inhibitory concentrations of the individual synthetic peptides against both *Bd* (Figure 4A; Supplementary Figure S2) and *Bsal* (Figure 4B; Supplementary Figure S3) is provided in Table 3. In general, the activities were greater against *Bd* than *Bsal*, and the ranatuerin peptides were more active than the brevinin peptides. In addition to the MIC, the minimum dose at which zoospore motility was lost and the minimum dose at which sporangia were no longer present upon microscopic examination were recorded. The brevinin peptides

inhibited the *Bd* zoospore motility at concentrations as low as 3.13 μM, but had MICs at 100 μM or higher than the measured range.

Pathogen diagnostics and microbiome of leopard frogs

Bd, but not *Bsal*, was detected in 8 of 10 Panamanian species, as summarized in Table 1. All 13 of the Ngäbe-Buglé leopard frogs sampled were infected, with a mean ± SD of $2.5 ± 9.6 × 10^6$ genome equivalents. This species had the highest prevalence and infection loads among those sampled.

Our analysis of the microbiomes of leopard frogs from North and Central America revealed a wide variability in the community composition of the skin bacteria (Figure 5). It was found that both species (non-parametric PERMANOVA: $F_{384,6} = 42.837$, $R^2 = 0.38$, $p < 0.001$) and site ($F_{384,5} = 42.837$, $R^2 = 0.37$, $p = 0.009$) were significant predictors of the leopard frog microbiomes. Seasonality played a significant, but lesser, role ($F_{384,3} = 42.837$, $R^2 = 0.05$, $p <$
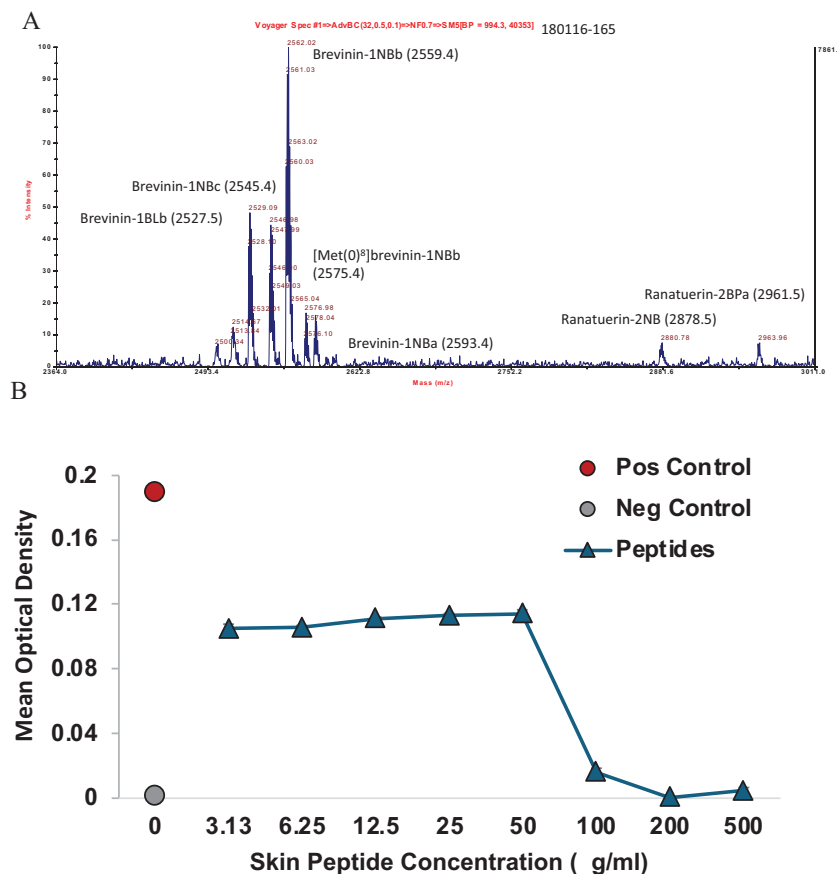

FIGURE 3
Natural mixtures of skin defense peptides from the Ngäbe-Buglé leopard frog. **(A)** Matrix-assisted laser desorption ionization time-of-flight (MALDI-TOF) mass spectrum of a representative frog (date-ID: 180116-165, *bottom panel*). See Supplementary Figure S1 for the MALDI spectra indicating undescribed peptides from additional amphibian species sampled at Altos de Piedra, Panama. **(B)** Optical density at 490 nm indicating the inhibition of growth of *Batrachochytrium dendrobatidis* at concentrations above 50 g/ml of natural mixtures of peptides. Data shown are representative of three replicate experiments.
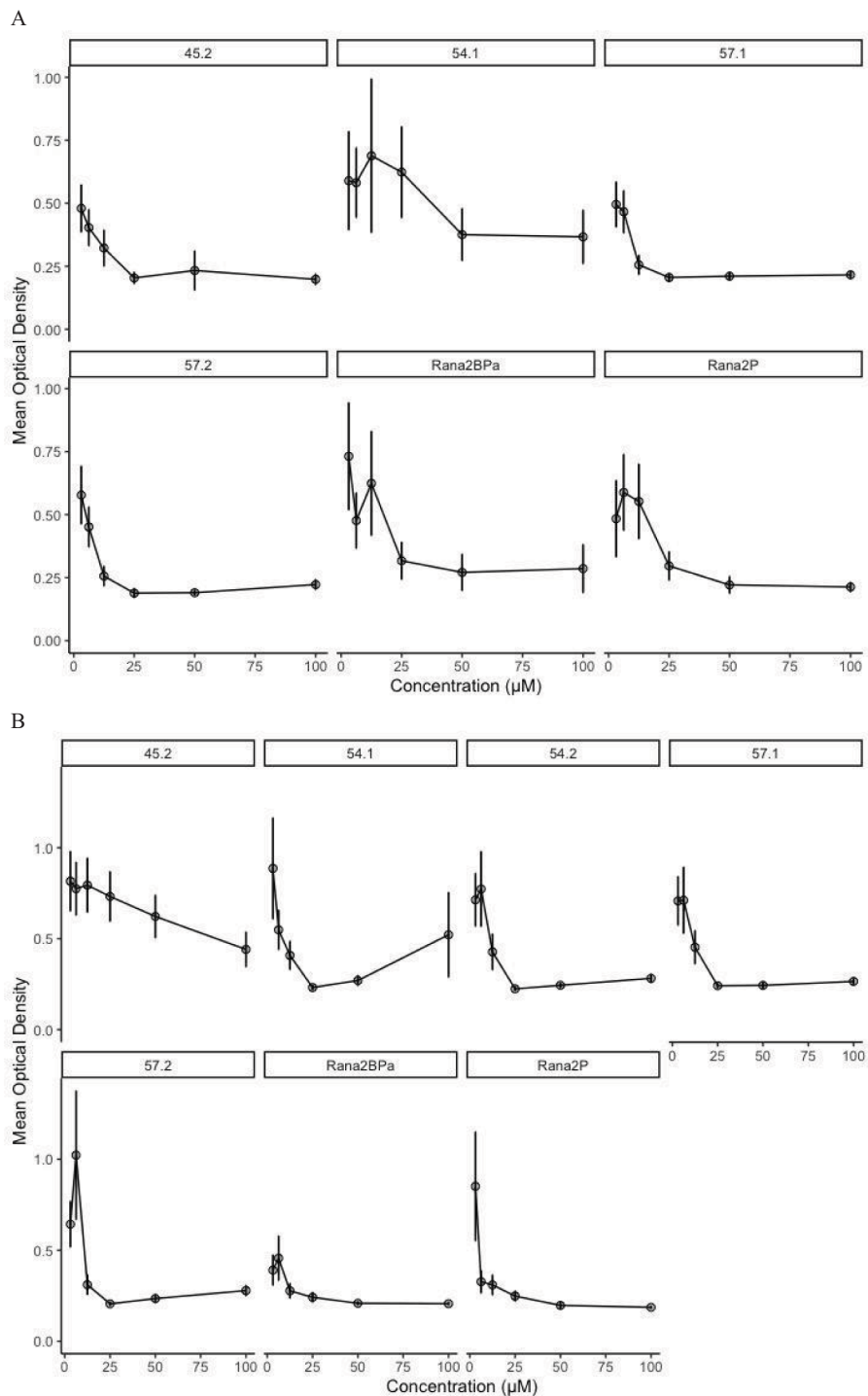
FIGURE 4
Pathogen inhibition by synthetic peptides. Optical density at 490 nm indicating the growth of *Batrachochytrium dendrobatidis* (*Bd*) **(A)** and *Batrachochytrium salamandrivorans* (*Bsal*) **(B)** after 7 days at given concentrations of peptide. Peptide names can be found in Table 2. See Supplementary Figures S2, S3 for the *Bd* and *Bsal* growth curves through time at each concentration of peptide.

0.001) in structuring the leopard frog microbiome. The sOTU richness differed significantly among species (Figure 6A). *R. warszewitschii* had the highest sOTU richness overall, with approximately 250 sOTUs, and had significantly higher richness than all species examined (Welch's *t*-test: Benjamini–Hochberg corrected *p*-values <0.05). The only other significant difference in

richness was that between *R. pipiens* from VT and the Ngäbe-Buglé leopard frog, with approximately 150 and 75 sOTUs, respectively. The proportion of the leopard frog microbiome inhibitory toward *Bd* was high across all species examined (Figure 6B). The Ngäbe-Buglé leopard frog had a significantly greater proportion of anti-*Bd* bacteria than the other species examined, except for the *L.*

TABLE 3 Minimal inhibitory concentration (MIC) at which peptides completely inhibit the growth and movement of *Batrachochytrium dendrobatidis* (*Bd*) or *B. salamandrivorans* (*Bsal*).

Peptide	*Batrachochytrium dendrobatidis*			*Batrachochytrium salamandrivorans*		
	MIC (μM)	Minimum Dose Lost Visual Zoospore Motility (μM)	Minimum Dose Lost Visual Sporangia (μM)	MIC (μM)	Minimum Dose Lost Visual Zoospore Motility (μM)	Minimum Dose Lost Visual Sporangia (μM)
Ranatuerin-2P control*	12.5	50	>100	12.5	100	>100
Ranatuerin-2BPa	25	100	100	6.25	100	100
Ranateurin-2NB	12.5	25	100	>100	100	>100
[Met(0)^8]brevinin-1NBb	not tested					
Brevinin-1NBa	>100	100	>100	>100	100	100
Brevinin-1NBb	100	3.13	6.25	>100	100	50
Brevinin-1BLb	>100	25	50	>100	100	>100
Brevinin-1NBc	>100	25	25	>100	100	50

Upon microscopic examination of the zoospore motility and presence of sporangia, the dose of peptide indicates the lowest dose at which visibility was lost.
*Ranatuerin-2P is not found in the Ngäbe-Buglé leopard frog, but is from *Rana pipiens* and was used for comparison to previous studies.

warszewitschii and *R. sphenocephala* from TN (Welch's *t*-test: Benjamini-Hochberg corrected *p*-values <0.05). No other significant differences in the *Bd* inhibitory taxa were observed.

Subsequently, the taxa that were important members of the microbiomes across the North American leopard frog populations and the Panamanian *R. warszewitschii* and Ngäbe-Buglé leopard frogs were examined by determining an occupancy abundance relationship (Figure 7), described above. Overall, 46 sOTUs were identified as being either in >50% of all leopard frog samples or with >15% abundance, suggesting that these taxa are important members of the leopard frog microbiome across seasons, species, and locations. Interestingly, of the 46 sOTUs, 29 were a >99% match to an isolate previously identified as being inhibitory toward *Bd*, suggesting that these taxa play an important role in host immune function (Supplementary Table S1).

Microbiome of Panamanian amphibians

There were no significant differences in sOTU richness (Figure 8A) among the amphibian species in Panama (Welch's *t*-test: Benjamini-Hochberg corrected *p*-values >0.05). The Ngäbe-Buglé leopard frog had among the lowest sOTU richness, with an average richness of 75 sOTUs per sample (SD ± 25.4). Minimal significant differences were observed in the proportion of the community with predicted inhibitory function against *Bd* (Figure 8B), ranging from 0% to 20% of the community. *Smilisca sila* had a significantly higher inhibitory abundance than *H. colymba*, the Ngäbe-Buglé leopard frog, and *L. warszewitschii* (Welch's *t*-test: Benjamini–Hochberg corrected *p*-values <0.05), with no other significant differences being noted. For the amphibians in Panama, significant effects were found in the community composition due to the amphibian species (non-parametric PERMANOVA: $F_{88,9}$ = 5.55, R^2 = 0.39, *p* < 0.001) (Figure 9). Significant effects of *Bd* abundance on the community composition were found as well, with axis 1 values

significantly correlating with the $\log_{10}$ abundance of *Bd* (Spearman's ρ = −0.55, *p* < 0.001). The taxa that were correlated with *Bd* load are described in Supplementary Table S2 (Spearman's correlation: Benjamini–Hochberg corrected *p*-values <0.05), which included five sOTUs thought to inhibit the growth of *Bd* found at higher abundance in frogs with lower infection loads: *Pseudomonas* sp., *Janthinobacterium lividum*, Enterobacteriaceae, Oxalobacteraceae, and *Pseudomonas fragi*. Many anti-*Bd* bacteria were also considered "core" bacteria across leopard frog species (Supplementary Table S1).
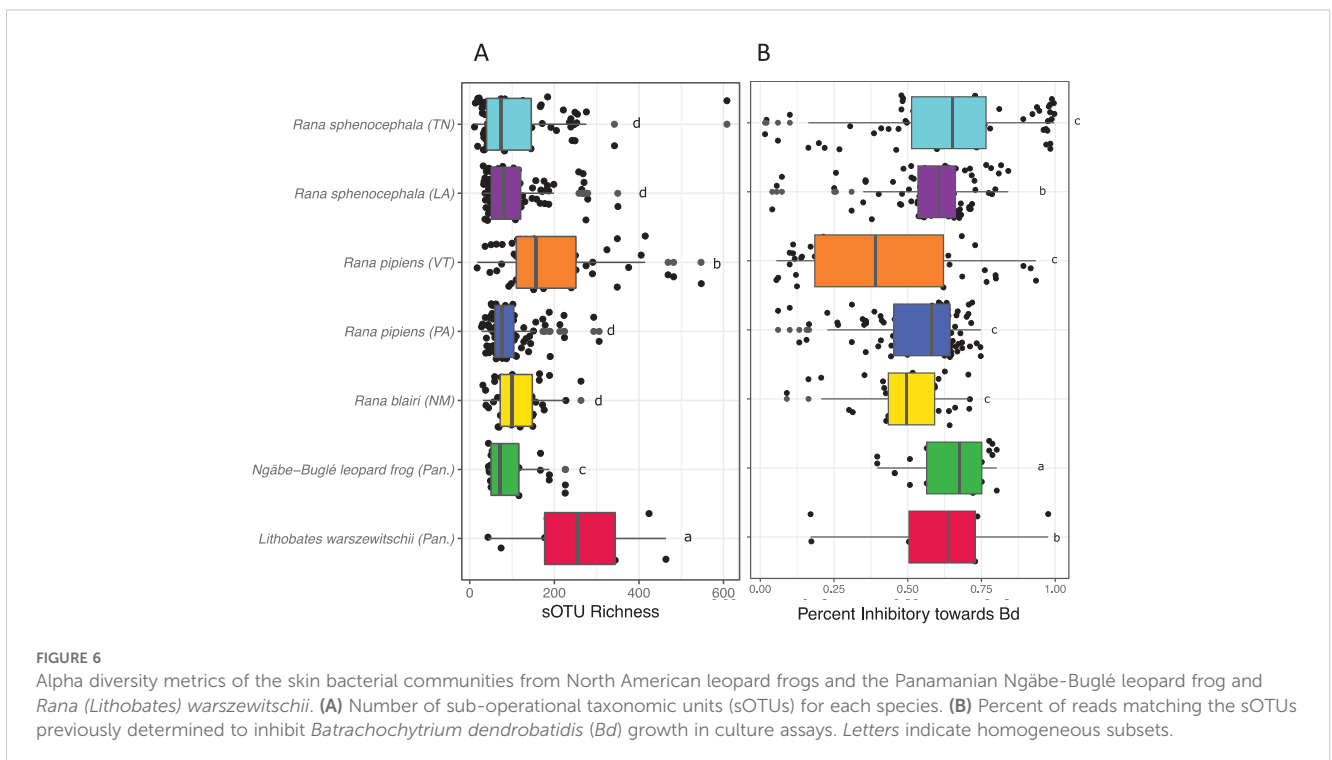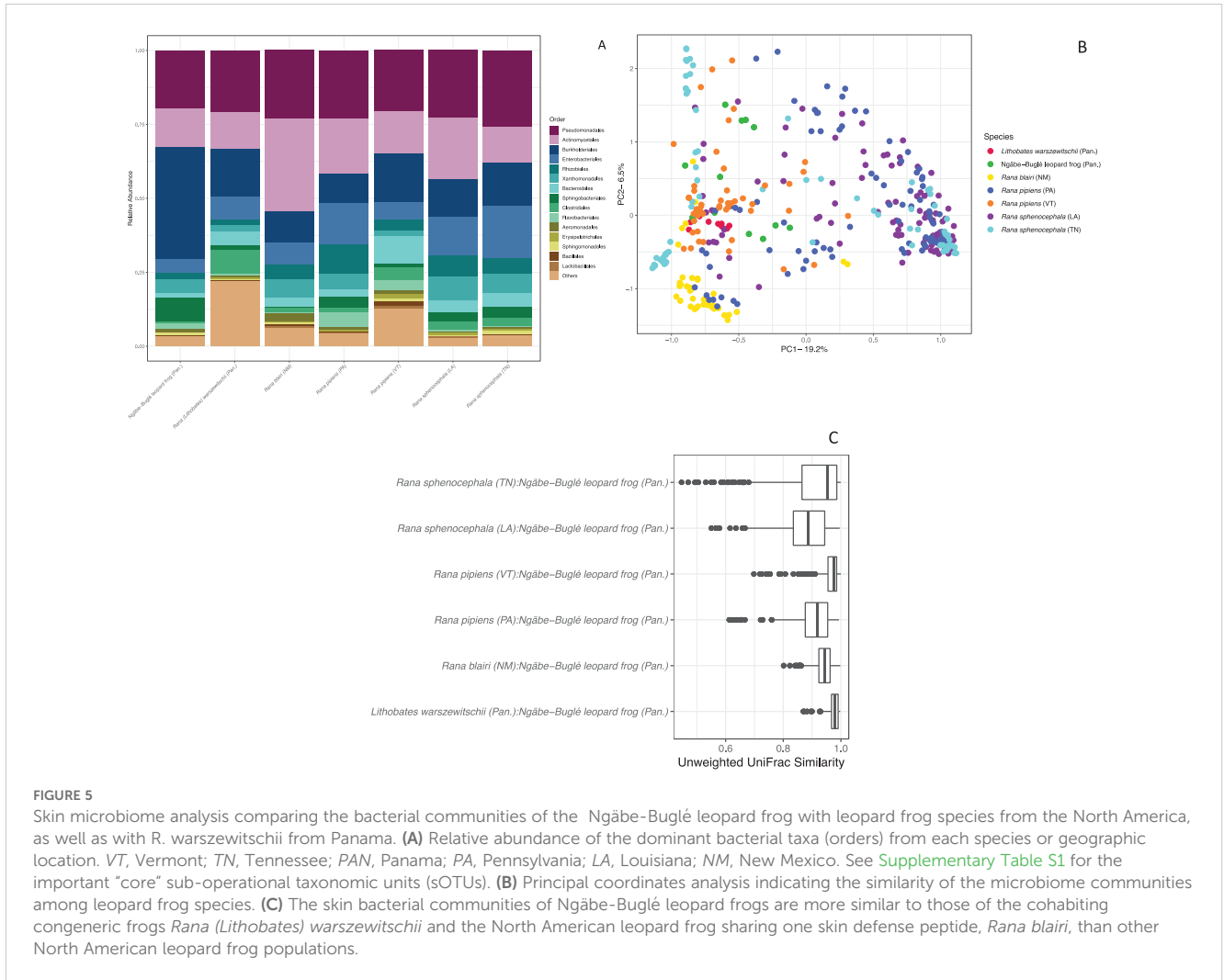
Discussion

Characterizing an understudied species

Museum specimens and field records indicate a distribution of the Ngäbe-Buglé leopard frog from Santa Fe to Buäbiti (Llano Tugrí) in the Comarca Ngäbe-Buglé, but genetic analysis and formal species description are ongoing. Additional information is needed on the calls and life history to taxonomically describe this species, as well as to monitor populations of this species that are potentially range-restricted and of conservation concern. The species range largely within the Comarca Ngäbe-Buglé endears a future species description honoring the indigenous people who live near these frogs, avoiding an imperialistic eponym (Guedes et al., 2023).

Skin peptides and leopard frog evolution

Characterizing the skin peptides from the Ngäbe-Buglé leopard frogs may help distinguish cryptic species from among *Pantherana*. Seven skin defense peptides were described, six of which have not previously been found. One peptide, brevinin-1BLb, was previously described from *R. blairi*, which was a minor component of skin

FIGURE 5
Skin microbiome analysis comparing the bacterial communities of the Ngäbe-Buglé leopard frog with leopard frog species from the North America, as well as with R. warszewitschii from Panama. **(A)** Relative abundance of the dominant bacterial taxa (orders) from each species or geographic location. *VT*, Vermont; *TN*, Tennessee; *PAN*, Panama; *PA*, Pennsylvania; *LA*, Louisiana; *NM*, New Mexico. See Supplementary Table S1 for the important "core" sub-operational taxonomic units (sOTUs). **(B)** Principal coordinates analysis indicating the similarity of the microbiome communities among leopard frog species. **(C)** The skin bacterial communities of Ngäbe-Buglé leopard frogs are more similar to those of the cohabiting congeneric frogs *Rana (Lithobates) warszewitschii* and the North American leopard frog sharing one skin defense peptide, *Rana blairi*, than other North American leopard frog populations.

FIGURE 6
Alpha diversity metrics of the skin bacterial communities from North American leopard frogs and the Panamanian Ngäbe-Buglé leopard frog and *Rana (Lithobates) warszewitschii*. **(A)** Number of sub-operational taxonomic units (sOTUs) for each species. **(B)** Percent of reads matching the sOTUs previously determined to inhibit *Batrachochytrium dendrobatidis* (*Bd*) growth in culture assays. *Letters* indicate homogeneous subsets.
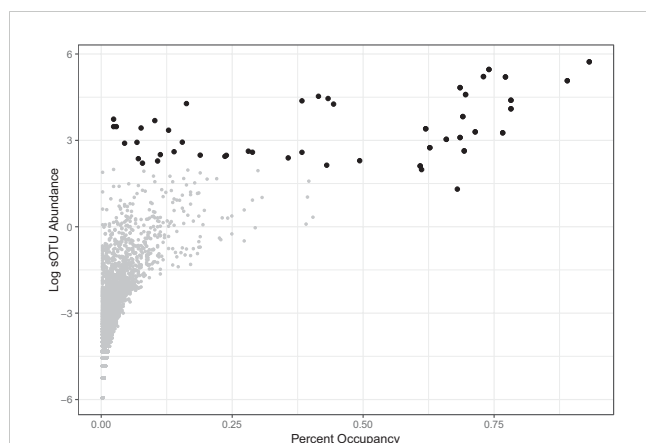
FIGURE 7
Important "core" sub-operational taxonomic units (sOTUs) identified from North American leopard frogs and the Panamanian Ngäbe-Buglé leopard frog and *Rana (Lithobates) warszewitschii.* Of the 46 core sOTUs defined as being either in >50% of all leopard frog samples or with >15% abundance, 29 were a >99% match to an isolate previously identified as being inhibitory toward *Batrachochytrium dendrobatidis* (*Bd*) (Supplementary Table S1).

secretions from that species and was not previously tested for cytolytic activity (Conlon et al., 2009a). Notably, we found that, aside from the congeneric species in Panama, the most similar microbiome structure to that of Ngäbe-Buglé leopard frogs was found in *R. blairi* (Figure 5C), indicating the role of skin defense peptides in the assemblage of microbiota.

We found one peptide in the Ngäbe-Buglé leopard frogs, ranatuerin-2BPa, which was predicted to occur in the common ancestor of the leopard frogs *R. pipiens* and *R. blairi* by Tennessen and Blouin (2010). This is a remarkable confirmation of an evolutionary hypothesis based on skin peptide sequences. The extant peptide ranaturin-2P and the ancestral peptide ranatuerin-

2BPa were not found to have differential activity against six tested bacterial pathogens of leopard frogs, although both peptides had antibacterial activity (Tennessen and Blouin, 2010). While this did not support the hypothesized selective sweep and rapid adaptive evolution of defensive peptides, fungi were not tested. Here, we found that the extant peptide in *R. pipiens* had a lower MIC against *Bd* than the ancestral peptide. Thus, we suggest that it is possible that *Bd* or another fungal pathogen may have been involved in the selective sweep of ranaturin-2P. However, the reverse pattern was found for the activity against *Bsal*, in which the ancestral peptide had a lower MIC (6.25 M) than either ranatuerin-2P (MIC = 12.5 M) or any of the other Ngäbe-Buglé leopard frog peptides (MICs >100 M). Thus, this ancestral peptide likely advantages the frogs against some fungal pathogens in the tropics, while the selective sweep may have favored the more active ranatuerin-2 peptides against fungal pathogens faced by the temperate *R. pipiens, R. sphenocephala*, and *R. blairi.* Tennessen and Blouin (2010) demonstrated that defense peptides can be used to investigate adaptive evolutionary patterns, and evolutionary changes may be ongoing in the current chytridiomycosis panzootic (Voyles et al., 2018). Indeed, populations of the northern leopard frog have distinctive skin peptide profiles that may be related to infection pressures or other local adaptations (Tennessen et al., 2009).

In addition to understanding evolutionary adaptations (Hanson, 2024), peptidomics have been used to distinguish among frogs in the European water frog hybridogenic complex (*Pelophylax esculentus* complex), consisting of *P. esculentus, Pelophylax lessonae*, and *Pelophylax ridibundus* (Daum et al., 2012). Peptidomic analysis of skin secretions may help differentiate cryptic species. Peptides have been used in evolutionary studies of North American Ranidae, including in the development of phylogenetic trees based on the amino acid sequences of the brevinin-1, rantuerin-2, and temporin peptides that support the split between *Lithobates* and *Rana* (Conlon et al., 2009b). However, one study found few differences in the peptide
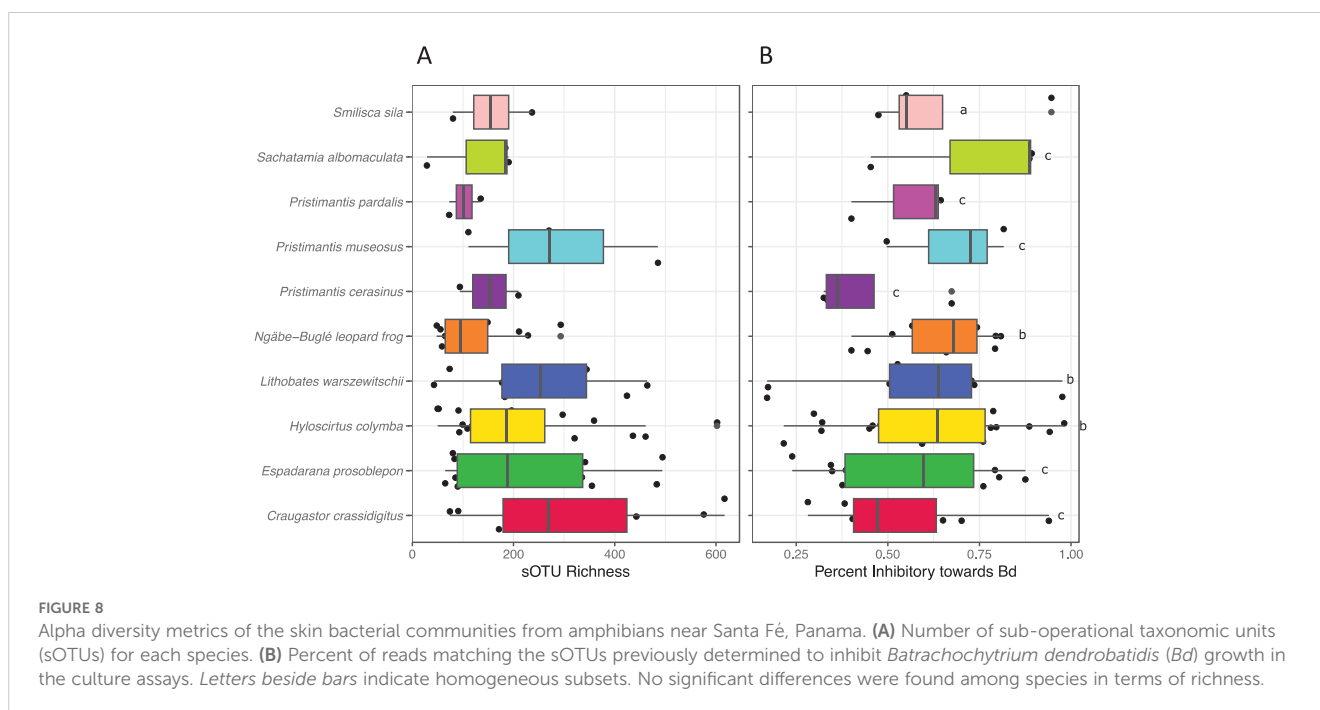

FIGURE 8
Alpha diversity metrics of the skin bacterial communities from amphibians near Santa Fé, Panama. **(A)** Number of sub-operational taxonomic units (sOTUs) for each species. **(B)** Percent of reads matching the sOTUs previously determined to inhibit *Batrachochytrium dendrobatidis* (*Bd*) growth in the culture assays. *Letters beside bars* indicate homogeneous subsets. No significant differences were found among species in terms of richness.
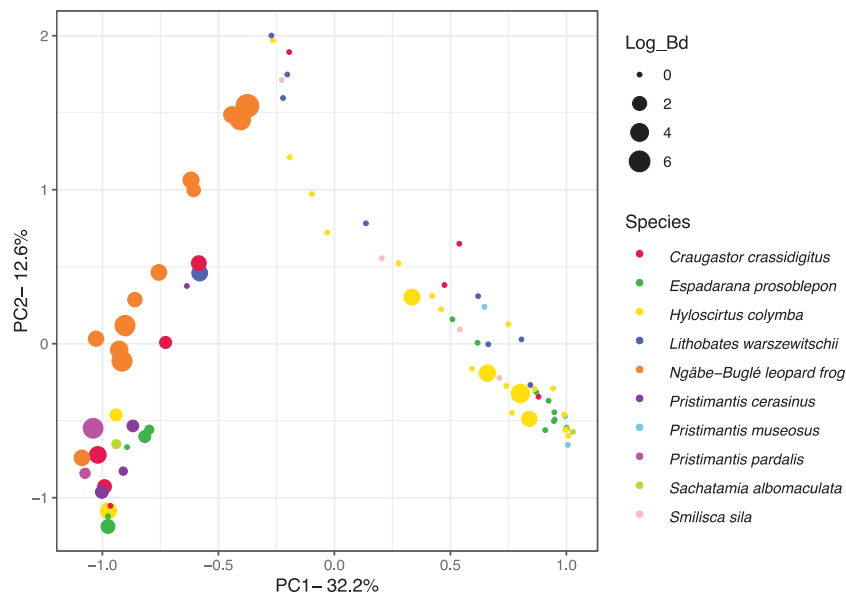
FIGURE 9
Principal coordinates analysis of the skin bacterial communities from amphibians near Santa Fé, Panama, with markers for individual frogs scaled by *Batrachochytrium dendrobatidis* (*Bd*) infection load. PC1 explains the difference between *Bd* infected and not infected, with the notable exception of *Hyloscirtus colymba*. Some *H. colymba* have high *Bd* loads, and this species disappeared for several years, but may now be recovering at Santa Fe (Sosa-Bartuano et al., 2023).

profiles distinguishing between the closely related *Rana muscosa* (Sixty-Lake Bain) and *Rana sierrae* (Conness Pond) (Woodhams et al., 2007). Nevertheless, we suggest that peptide profiles be incorporated into future phylogenetic analyses that include the Ngäbe-Buglé leopard frogs and other Central American Ranidae, along with genetic, morphometric, and acoustic analyses. Further description of the larvae (Figure 2) and the life history characteristics among Panamanian Ranidae may also be informative and help determine disease risk, although related species including *R. pipiens* larvae appear to be resistant to *Bd* infections (Wilber et al., 2022).

Contribution of skin peptide defenses and microbiome to anti-*Bd* defense

The anti-*Bd* proportion of the microbiome did not correlate significantly with the anti-*Bd* activity of the mucosome for all the Panama frog samples analyzed together, nor for the Ngäbe-Buglé leopard frogs analyzed separately. Thus, we suggest that skin defense peptides play a larger role than constitutive skin defenses, at least for species that express such peptides, including the Ngäbe-Buglé leopard frog and several other species persisting at Alto de Piedra (Supplementary Figure S1). We note that recent improvements in the mucosome collection and analysis methods (NM and DCW, unpublished data) are suggested for future studies, including a shorter soak time (30 min) in 12.5 ml artificial pond water (or stream water for sensitive tadpoles) frozen in a 15-ml tube (not filled completely to prevent cracking during freezing), and then lyophilized to a powder and rehydrated at a volume corresponding to a body size correction factor. That said, a previous study indicated that *E. prosoblepon* had particularly effective peptides against *Bd*

(Woodhams et al., 2006), which was one of the few frogs to maintain populations after declines through an epizootic at El Copé, Panama, and had relatively low infection burden and prevalence compared with other species (Longo et al., 2023). One notable species, *H. colymba*, which disappeared and may now be recovering, had high *Bd* loads but similar bacterial communities to those of uninfected frogs, as well as a complex mixture of undescribed skin peptides. Natural product discovery focused on these persisting species, particularly the description of the skin defense peptides from hosts and the potential antibiotic metabolites produced by amphibian skin microbiota (Martin H et al., 2020), is likely to advance our understanding of disease defense. The functions of the mucosome are not completely understood, and the roles of chemo-attractants or repellents against infectious zoospores (Moss et al., 2008; Wang et al., 2021), as well as the impact on infection tolerance or disease development, are characteristics not measured by pathogen growth assays. Beyond aqueous secondary metabolites acting as antifungals, volatile organic compounds, biofilms, and other features of interacting microbes likely impact the functions of the mucosome and likely interact with skin defense peptides.

Effectiveness of individual amphibian antimicrobial peptides against *Bd* and *Bsal*

The examination of MICs against both *Bd* and *Bsal* provides insights into the pathogen inhibition properties of the novel peptides from the Ngäbe-Buglé leopard frog. The data consistently demonstrated lower concentrations of the peptides needed to inhibit *Bd* than *Bsal*, not only from the optical density measurements of growth but also from the analysis of zoospore motility and sporangia

formation. The ranatuerin-2 peptides exhibited the most potent inhibition against *Bd* (12.5 µM) and *Bsal* (3.13 µM), outperforming the brevinin-1 family peptides. The brevinin-1 peptides had notable activity against *Bd* zoospore motility (Table 3).

These findings imply that skin peptides contribute to the defense or infection tolerance, in addition to the regulation of the skin microbiome, of the Ngäbe-Buglé leopard frog. Understanding the inhibitory effects of distinct peptides at varying concentrations contributes to our ability to develop targeted strategies for protecting vulnerable amphibian populations at critical field sites. Our data also suggest that, to limit the pathogen pressure on amphibians at Alto de Piedra, management efforts focused on reducing the pathogen loads particularly on adult Ngäbe-Buglé leopard frogs may provide a strategic benefit. Studies examining the *Bd* isolates from these frogs could also provide insights, although to date only members of the global panzootic lineage-2 subclade have been detected in Panama, indicative of a recent invasion (Rothstein et al., 2021). An alternative to reducing the pathogen load on supershedding hosts is to investigate the skin microbes noted to be associated with either resistance or tolerance to the *Bd* in this study (Supplementary Table S2), including *Pseudomonas* spp., *J. lividum*, and *Sanguibacter* spp., and others that make up a "core microbiome" on the skin of persisting populations of leopard frogs (Supplementary Table S1). Some of these have not yet been cultured, while others such as *J. lividum* are well known for their beneficial skin probiotic applications (Harris et al., 2009; Kueneman et al., 2016).

Data availability statement

The original contributions presented in the study are publicly available. This data can be found here: NCBI Sequence Read Archive, accession PRJNA1175825, PRJNA1177182.

Ethics statement

The animal study was approved by University of Massachusetts Boston IACUC and the Ministerio de Ambiente (MiAmbiente) of the República de Panamá. The study was conducted in accordance with the local legislation and institutional requirements.

Author contributions

DW: Conceptualization, Data curation, Formal analysis, Funding acquisition, Investigation, Methodology, Project administration, Resources, Supervision, Writing – original draft, Writing – review & editing. AM-T: Data curation, Formal analysis, Investigation, Methodology, Visualization, Writing – original draft, Writing – review & editing. AH: Data curation, Funding acquisition, Investigation, Methodology, Writing – original draft, Writing – review & editing. PK: Formal analysis, Visualization, Writing – original draft, Writing – review & editing. NM: Formal analysis, Methodology, Writing – original draft, Writing – review &

editing. LR: Data curation, Formal analysis, Investigation, Visualization, Writing – original draft, Writing – review & editing. LR-S: Funding acquisition, Supervision, Writing – original draft, Writing – review & editing. BL: Data curation, Formal analysis, Methodology, Visualization, Writing – original draft, Writing – review & editing. JV: Funding acquisition, Investigation, Writing – original draft, Writing – review & editing. CR-Z: Funding acquisition, Investigation, Writing – original draft, Writing – review & editing. DC: Visualization, Writing – original draft, Writing – review & editing. JC: Formal analysis, Investigation, Methodology, Visualization, Writing – original draft, Writing – review & editing.

Conflict of interest

The authors declare that the research was conducted in the absence of any commercial or financial relationships that could be construed as a potential conflict of interest.

Publisher's note

All claims expressed in this article are solely those of the authors and do not necessarily represent those of their affiliated organizations, or those of the publisher, the editors and the reviewers. Any product that may be evaluated in this article, or claim that may be made by its manufacturer, is not guaranteed or endorsed by the publisher.

Supplementary material

The Supplementary Material for this article can be found online at: https://www.frontiersin.org/articles/10.3389/famrs.2024.1458731/full#supplementary-material

References

Amir, A., McDonald, D., Navas-Molina, J. A., Kopylova, E., Morton, J. T., Zech Xu, Z., et al. (2017). Deblur rapidly resolves single-nucleotide community sequence patterns. *mSystems* 2, e00191–e00116. doi: 10.1128/mSystems.00191-16

Assis, A. B., Barreto, C. C., and Navas, C. A. (2017). Skin microbiota in frogs from the Brazilian Atlantic Forest: Species, forest type, and potential against pathogens. *PLoS One* 12, e0179628. doi: 10.1371/journal.pone.0179628

Assis, V. R., Robert, J., and Titon, S. C. M. (2023). Introduction to the special issue Amphibian immunity: stress, disease and ecoimmunology. *Philos. Trans. R Soc. Lond B Biol. Sci.* 378, 20220117. doi: 10.1098/rstb.2022.0117

Blooi, M., Pasmans, F., Longcore, J. E., Spitzen-van der Sluijs, A., Vercammen, F., and Martel, A. (2013). Duplex real-time PCR for rapid simultaneous detection of *Batrachochytrium dendrobatidis* and *Batrachochytrium salamandrivorans* in amphibian samples. *J. Clin. Microbiol.* 51, 4173–4177. doi: 10.1128/JCM.02313-13

Bolyen, E., Rideout, J. R., Dillon, M. R., Bokulich, N. A., Abnet, C. C., Al-Ghalith, G. A., et al. (2019). Reproducible, interactive, scalable and extensible microbiome data science using QIIME 2. *Nat. Biotechnol.* 37, 852–857. doi: 10.1038/s41587-019-0209-9

Brem, F. M. R., and Lips, K. R. (2008). *Batrachochytrium dendrobatidis* infection patterns among Panamanian amphibian species, habitats and elevations during epizootic and enzootic stages. *Dis. Aquat. Org.* 81, 189–202. doi: 10.3354/dao01960

Brunetti, A. E., Lyra, M. L., Bauermeister, A., Bunk, B., Boedeker, C., Müsken, M., et al. (2023). Host macrocyclic acylcarnitines mediate symbiotic interactions between frogs and their skin microbiome. *iScience.* 26, 108–109. doi: 10.1016/j.isci.2023.108109

Caporaso, J. G., Lauber, C. L., Walters, W. A., Berg-Lyons, D., Huntley, J., Fierer, N., et al. (2012). Ultra-high-throughput microbial community analysis on the Illumina HiSeq and MiSeq platforms. *ISME J.* 6, 1621–1624. doi: 10.1038/ismej.2012.8

Castro Monzon, F., Rödel, M.-O., Ruland, F., Parra-Olea, G., and Jeschke, J. M. (2022). *Batrachochytrium salamandrivorans'* amphibian host species and invasion range. *EcoHealth* 19, 475–486. doi: 10.1007/s10393-022-01620-9

Catenazzi, A., Swei, A., Finkle, J., Foreyt, E., Wyman, L., and Vredenburg, V. T. (2017). Epizootic to enzootic transition of a fungal disease in tropical Andean frogs: Are surviving species still susceptible? *PLoS One* 12, e0186478. doi: 10.1371/journal.pone.0186478

Conlon, J. M. (2008). Reflections on a systematic nomenclature for antimicrobial peptides from the skins of frogs of the family Ranidae. *Peptides* 29, 1815–1819. doi: 10.1016/j.peptides.2008.05.029

Conlon, J. M., Ahmed, E., Coquet, L., Jouenne, T., Leprince, J., Vaudry, H., et al. (2009a). Peptides with potent cytolytic activity from the skin secretions of the North American leopard frogs, *Lithobates blairi* and *Lithobates yavapaiensis. Toxicon* 53, 699–705. doi: 10.1016/j.toxicon.2009.02.018

Conlon, J. M., Kolodziejek, J., and Nowotny, N. (2009b). Antimicrobial peptides from the skins of North American frogs. *Biochim. Biophys. Acta (BBA) - Biomembranes* 1788, 1556–1563. doi: 10.1016/j.bbamem.2008.09.018

Crawford, A. J., Lips, K. R., and Bermingham, E. (2010). Epidemic disease decimates amphibian abundance, species diversity, and evolutionary history in the highlands of central Panama. *PNAS* 107, 13777–13782. doi: 10.1073/pnas.0914115107

Daum, J. M., Davis, L. R., Bigler, L., and Woodhams, D. C. (2012). Hybrid advantage in skin peptide immune defenses of water frogs (*Pelophylax esculentus*) at risk from emerging pathogens. *Infect. Genet. Evol.* 12, 1854–1864. doi: 10.1016/j.meegid.2012.07.024

Dixon, P. (2003). VEGAN, a package of R functions for community ecology. *J. Veget. Sci.* 14, 927–930. doi: 10.1111/j.1654-1103.2003.tb02228.x

Gray, M. J., Carter, E. D., Piovia-Scott, J., Cusaac, J. P. W., Peterson, A. C., Whetstone, R. D., et al. (2023). Broad host susceptibility of North American amphibian species to *Batrachochytrium salamandrivorans* suggests high invasion potential and biodiversity risk. *Nat. Commun.* 14, 3270. doi: 10.1038/s41467-023-38979-4

Guedes, P., Alves-Martins, F., Arribas, J. M., Chatterjee, S., Santos, A. M. C., Lewin, A., et al. (2023). Eponyms have no place in 21st-century biological nomenclature. *Nat. Ecol. Evol.* 7, 1157–1160. doi: 10.1038/s41559-023-02022-y

Hanson, M. A. (2024). When the microbiome shapes the host: immune evolution implications for infectious disease. *Phil. Trans. R. Soc B* 379, 20230061. doi: 10.1098/rstb.2023.0061

Harris, R. N., Brucker, R. M., Walke, J. B., Becker, M. H., Schwantes, C. R., Flaherty, D. C., et al. (2009). Skin microbes on frogs prevent morbidity and mortality caused by a lethal skin fungus. *ISME J.* 3, 818–824. doi: 10.1038/ismej.2009.27

Hillis, D. M., and Wilcox, T. P. (2005). Phylogeny of the New World true frogs (*Rana*). *Molec. Phylogen. Evol.* 34, 299–314. doi: 10.1016/j.ympev.2004.10.007

Hollanders, M., Grogan, L. F., Nock, C. J., McCallum, H. I., and Newell, D. A. (2023). Recovered frog populations coexist with endemic *Batrachochytrium dendrobatidis* despite load-dependent mortality. *Ecol. Appl.* 33, e2724. doi: 10.1002/eap.2724

Kueneman, J. G., Woodhams, D. C., Harris, R., Archer, H. M., Knight, R., and McKenzie, V. J. (2016). Probiotic treatment restores protection against lethal fungal infection lost during amphibian captivity. *Proc. R. Soc B.* 283, 20161553. doi: 10.1098/rspb.2016.1553

Le Sage, E. H., LaBumbard, B. C., Reinert, L. K., Miller, B. T., Richards-Zawacki, C. L., Woodhams, D. C., et al. (2021). Preparatory immunity: Seasonality of mucosal skin defences and *Batrachochytrium* infections in Southern leopard frogs. *J. Anim. Ecol.* 90, 542–554. doi: 10.1111/1365-2656.13386

Lips, K. R. (2016). Overview of chytrid emergence and impacts on amphibians. *Phil. Trans. R. Soc B* 371, 20150465. doi: 10.1098/rstb.2015.0465

Lips, K. R., Brem, F., Brenes, R., Reeve, J. D., Alford, R. A., Voyles, J., et al. (2006). Emerging infectious disease and the loss of biodiversity in a Neotropical amphibian community. *PNAS* 103, 3165–3170. doi: 10.1073/pnas.0506889103

Longo, A. V., Lips, K. R., and Zamudio, K. R. (2023). Evolutionary ecology of host competence after a chytrid outbreak in a naive amphibian community. *Phil. Trans. R. Soc B* 378, 20220130. doi: 10.1098/rstb.2022.0130

Lozupone, C., and Knight, R. (2005). UniFrac: a new phylogenetic method for comparing microbial communities. *Appl. Environ. Micro.* 71, 8228–8235. doi: 10.1128/AEM.71.12.8228-8235.2005

Luque-Montes, I., Austin, J. D., Weinfurther, K. D., Wilson, L. D., Hofmann, E. P., and Townsend, J. H. (2018). An integrative assessment of the taxonomic status of putative hybrid leopard frogs (Anura: Ranidae) from the Chortís Highlands of Central America, with description of a new species. *System. Biodiv.* 16, 340–356. doi: 10.1080/14772000.2017.1415232

Martin H., C., Ibáñez, R., Nothias, L.-F., Caraballo-Rodríguez, A. M., Dorrestein, P. C., and Gutiérrez, M. (2020). Metabolites from microbes isolated from the skin of the Panamanian rocket frog *Colostethus Panamansis* (Anura: Dendrobatidae). *Metabolites* 10, 406. doi: 10.3390/metabo10100406

McDonald, D., Price, M. N., Goodrich, J., Nawrocki, E. P., DeSantis, T. Z., Probst, A., et al. (2012). An improved Greengenes taxonomy with explicit ranks for ecological and evolutionary analyses of bacteria and archaea. *ISME J.* 6, 610–618. doi: 10.1038/ismej.2011.139

Moss, A. S., Reddy, N. S., Dortaj, I. M., and San Francisco, M. J. (2008). Chemotaxis of the amphibian pathogen *Batrachochytrium dendrobatidis* and its response to a variety of attractants. *Mycologia* 100, 1–5. doi: 10.1080/15572536.2008.11832493

Myers, C. W., and Duellman, W. E. (1982). A new species of *Hyla* from Cerro Colorado, and other tree frog records and geographical notes from western Panama. *Am. Mus. Nov.* 2752, 1–32.

Newman, C. E., Feinberg, J. A., Rissler, L. J., Burger, J., and Shaffer, H. B. (2012). A new species of leopard frog (Anura: Ranidae) from the urban northeastern US. *Molec. Phylogen. Evol.* 63, 445–455. doi: 10.1016/j.ympev.2012.01.021

Parada, A. E., Needham, D. M., and Fuhrman, J. A. (2016). Every base matters: assessing small subunit rRNA primers for marine microbiomes with mock communities, time series and global field samples. *Environ. Microbiol.* 18, 1403–1414. doi: 10.1111/1462-2920.13023

Pask, J. D., Woodhams, D. C., and Rollins-Smith, L. A. (2012). The ebb and flow of antimicrobial skin peptides defends northern leopard frogs (*Rana pipiens*) against chytridiomycosis. *Global Change Biol.* 18, 1231–1238. doi: 10.1111/j.1365-2486.2011.02622.x

Pfeiler, E., and Markow, T. A. (2008). Phylogenetic relationships of leopard frogs (*Rana pipiens* complex) from an isolated coastal mountain range in southern Sonora, Mexico. *Molec. Phylogen. Evol.* 49, 343–348. doi: 10.1016/j.ympev.2008.06.011

Pfenning-Butterworth, A., Buckley, L. B., Drake, J. M., Farner, J. E., Farrell, M. J., Gehman, A.-L. M., et al. (2024). Interconnecting global threats: climate change, biodiversity loss, and infectious diseases. *Lancet* 8, e270–e283. doi: 10.1016/S2542-5196(24)00021-4

Rognes, T., Flouri, T., Nichols, B., Quince, C., and Mahé, F. (2016). VSEARCH: A versatile open source tool for metagenomics. *PeerJ* 4, e2584. doi: 10.7717/peerj.2584

Rohr, J. R., Sack, A., Bakhoum, S., Barrett, C. B., Lopez-Carr, D., Chamberlin, A. J., et al. (2023). A planetary health innovation for disease, food and water challenges in Africa. *Nature* 619, 782–787. doi: 10.1038/s41586-023-06313-z

Rollins-Smith, L. A., Carey, C., Longcore, J., Doersam, J. K., Boutte, A., Bruzgal, J. E., et al. (2002). Activity of antimicrobial skin peptides from ranid frogs against *Batrachochytrium dendrobatidis*, the chytrid fungus associated with global amphibian declines. *Dev. Comp. Immunol.* 26, 471–479. doi: 10.1016/S0145-305X(01)00088-X

Rothstein, A. P., Byrne, A. Q., Knapp, R. A., Briggs, C. J., Voyles, J., Richards-Zawacki, C. L., et al. (2021). Divergent regional evolutionary histories of a devastating global amphibian pathogen. *Proc. R. Soc B.* 288, 20210782. doi: 10.1098/rspb.2021.0782

Ruiz, V. L., and Robert, J. (2023). The amphibian immune system. *Phil. Trans. R. Soc B* 378, 20220123. doi: 10.1098/rstb.2022.0123

Scheele, B. C., Pasman, F., Skerratt, L. F., Berger, L., Martel, A., Beukema, W., et al. (2019). Amphibian fungal panzootic causes catastrophic and ongoing loss of biodiversity. *Science.* 363(6434), 1459–1463. doi: 10.1126/science.aav0379

Sosa-Bartuano, Á., Samudio, R. Jr., Carrión De Samudio, J., and Toribio, E. (2023). Notes on the natural history of the endangered La Loma Treefrog, *Hyloscirtus colymba* (Anura: Hylidae), from Santa Fe National Park, Panamá. *RandA* 30, e17783. doi: 10.17161/randa.v30i1.17783

Tennessen, J. A., and Blouin, M. S. (2010). A revised leopard frog phylogeny allows a more detailed examination of adaptive evolution at ranatuerin-2 antimicrobial peptide loci. *Immunogen.* 62, 333–343. doi: 10.1007/s00251-010-0430-7

Tennessen, J. A., Woodhams, D. C., Chaurand, P., Reinert, L. K., Billheimer, D., Shyr, Y., et al. (2009). Variations in the expressed antimicrobial peptide repertoire of northern leopard frog (*Rana pipiens*) populations suggest intraspecies differences in resistance to pathogens. *Dev. Comp. Immunol.* 33, 1247–1257. doi: 10.1016/j.dci.2009.07.004

Thompson, L. R., Sanders, J. G., McDonald, D., Amir, A., Ladau, J., Locey, K. J., et al. (2017). A communal catalogue reveals Earth's multiscale microbial diversity. *Nature* 551, 457–463. doi: 10.1038/nature24621

Valenzuela-Sánchez, A., Schmidt, B. R., Uribe-Rivera, D. E., Costas, F., Cunningham, A. A., and Soto-Azat, C. (2017). Cryptic disease-induced mortality may cause host extinction in an apparently stable host–parasite system. *Proc. R. Soc B.* 284, 20171176. doi: 10.1098/rspb.2017.1176

Voyles, J., Woodhams, D. C., Saenz, V., Byrne, A. Q., Perez, R., Rios-Sotelo, G., et al. (2018). Shifts in disease dynamics in a tropical amphibian assemblage are not due to pathogen attenuation. *Science* 359, 1517–1519. doi: 10.1126/science.aao4806

Wake, D. B., and Vredenburg, V. T.. (2008). Wake Colloquium paper: are we in the midst of the sixth mass extinction? A view from the world of amphibians. *Proc. Natl. Acad. Sci. U. S. A.* 105, 11466–11473. doi: 10.1073/pnas.0801921105

Wang, Y., Verbrugghe, E., Meuris, L., Chiers, K., Kelly, M., Strubbe, D., et al. (2021). Epidermal galactose spurs chytrid virulence and predicts amphibian colonization. *Nat. Commun.* 12, 5788. doi: 10.1038/s41467-021-26127-9

Wilber, M. Q., Ohmer, M. E. B., Altman, K. A., Brannelly, L. A., LaBumbard, B. C., Le Sage, E. H., et al. (2022). Once a reservoir, always a reservoir? Seasonality affects the pathogen maintenance potential of amphibian hosts. *Ecology* 103, e3759. doi: 10.1002/ecy.3759

Woodhams, D. C., Alford, R. A., Antwis, R. E., Archer, H., Becker, M. H., Belden, L. K., et al. (2015). Antifungal isolates database of amphibian skin-associated bacteria and function against emerging fungal pathogens: Ecological Archives E096-059. *Ecology* 96, 595–595. doi: 10.1890/14-1837.1

Woodhams, D. C., Barnhart, K., Bletz, M. C., Campos, A., Ganem, S. J., Hertz, A., et al. (2018). Batrachochytrium*: biology and management of a fungal pathogen of amphibians* (Chichester: eLS. John Wiley & Sons, Ltd). doi: 10.1002/9780470015902.a0027207

Woodhams, D. C., Bell, S. C., Bigler, L., Caprioli, R. M., Chaurand, P., Lam, B. A., et al. (2016). Life history linked to immune investment in developing amphibians. *Conserv. Physiol.* 4, cow025. doi: 10.1093/conphys/cow025

Woodhams, D. C., Boyle, D. G., Hyatt, A. D., and Rollins-Smith, L. A. (2008). The northern leopard frog *Rana pipiens* is a widespread reservoir species harboring *Batrachochytrium dendrobatidis* in North America. *Herp. Rev.* 39, 66–68.

Woodhams, D. C., Baumgartner, S., Kielgast, J., Kuepfer, E., Tobler, U., et al. (2014). Interacting symbionts and immunity in the amphibian skin mucosome predict disease risk and probiotic effectiveness. *PLoS One* 9, e96375. doi: 10.1371/journal.pone.0096375

Woodhams, D. C., Voyles, J., Lips, K. R., Carey, C., and Rollins-Smith, L. A. (2006). Predicted disease susceptibility in a Panamanian amphibian assemblage based on skin peptide defenses. *J. Wildl. Dis.* 42, 207–218. doi: 10.7589/0090-3558-42.2.207

Woodhams, D. C., Vredenburg, V. T., Simon, M.-A., Billheimer, D., Shakhtour, B., Shyr, Y., et al. (2007). Symbiotic bacteria contribute to innate immune defenses of the threatened mountain yellow-legged frog, *Rana muscosa*. Biol. *Cons.* 138, 390–398. doi: 10.1016/j.biocon.2007.05.004

Yuan, Z.-Y., Zhou, W.-W., Chen, X., Poyarkov, N. A., Chen, H.-M., Jang-Liaw, N.-H., et al. (2016). Spatiotemporal diversification of the true frogs (genus *Rana*): A historical framework for a widely studied group of model organisms. *Syst. Biol.* 65, 824–842. doi: 10.1093/sysbio/syw055